Proceedings of the Research Institute of Atmospherics,
Nagoya University, vol. 29 (1982) – Technical Report –

A DESIGN STUDY AND SOME EXPERIMENTS OF DIGITAL CORRELATOR BACKEND FOR λ 8-CM RADIOHELIOGRAPH AT TOYOKAWA

Masanori NISHIO, Yoshio TSUKIJI, Shinzo ENOME,
Kiyoto SHIBASAKI, and Koh-Ichiro MORITA

Abstract

A project is proposed to improve the time resolution and the dynamic range of the λ 8-cm radioheliograph system at Toyokawa. The main task of this project is to replace the backend of the present λ 8-cm radioheliograph with a digital correlator backend. By this improvement, a maximum time resolution of 0.1 sec./image with a minimum detectable flux of about 0.5 s.f.u. is expected. A design study of the digital correlator backend is executed. From the study and some experiments using a one-bit correlator, it becomes clear that a one-bit correlator is suitable for the digital correlator backend.

1. Introduction

The λ 8-cm radioheliograph at Toyokawa has been working since 1975 (Ishiguro et al., 1975), operating together with the λ 3-cm radioheliograph (Tanaka et al., 1970) and the fully-automatic radiopolarimeters (Torii et al., 1979) at Toyokawa in studying solar radio physics (Shibasaki et al., 1976, 1978; Ishiguro et al, 1980). The geometrical antenna configuration is a T-shaped array of 3-mϕ paraboloids, which consists of 32+2 elements on E-W baseline and of 16+2 elements on the N-S baseline. Five antenna combinations are

available in the following forms: E-W 32-element grating (HPBW=38', HPBW: Half Power Beam Width), E-W (32+2)-element compound (HPBW=1.25'), N-S 16-element grating (HPBW=2.5'), N-S (16+2)-element compound (HPBW=1.25'), and (32+16)-element pencil beam (HPBW=2.5'×2.5' cosZD, ZD: Zenith Distance) interferometers.

A project to improve the sensitivity and the phase stability of the system was undertaken in 1978 and 1979 (Ishiguro et al., 1979). At present, the design goal of the project, which was less than 1000K in receiver noise temperature and 5° rms/month in phase stability, has been achieved (Naito, 1979; Itoh and Torii, 1981).

In the present system, microwave signals received by each antenna are amplified and frequency-converted by a front-end receiver placed in close vicinity of each antenna, and transmitted independently to 2nd IF stage. Solar brightness distribution is observed by scanning with a fan beam or a pencil beam. Although a scanning interferometer with a fan beam or a pencil beam is very simple in its receiving system, it cannot assign as much integration time to each picture point as other types of interferometer, such as a multi-beam or multi-correlation (Fourier-synthesis) system. Therefore it has lower time resolution than that of the other systems. On the other hand, most impulsive microwave bursts have a short duration ranging between 1 and 10 minutes, and sometimes have a duration of only a few seconds. Therefore the present system does not have high enough time resolution to be able to observe such a fast event.

Following the previous project, it has been proposed to expand the λ 8-cm radioheliograph into a multi-correlation system in order to overcome the above-mentioned disadvantage. Through this project, time resolution can be drastically improved, and the λ 8-cm radioheliograph becomes a real time solar radiotelescope. This project is the last stage of the improvements to be made on the λ 8-cm radioheliograph. The main task of this project is to replace the backend of the present system with digital correlator backend. In a multi-correlation system, a large number of correlators are needed. The digital correlator is better than the analog one in point of its compactness and reproducibility. As the correlator to be used in the new backend, the one-bit correlator was considered and some experiments performed on it. In this note, we describe a design of the proposed system and some experiments associated with one-bit correlator of the new backend.

2. Design Study for Digital Correlator Backend

Figure 1 shows the block diagram of the new system. Microwave signals received by each antenna are independently amplified, frequency-converted, and then transmitted to the observation house in the vicinity of the array. The signals are digitized by A/D converter, and cross-correlated to produce spatial frequency components of

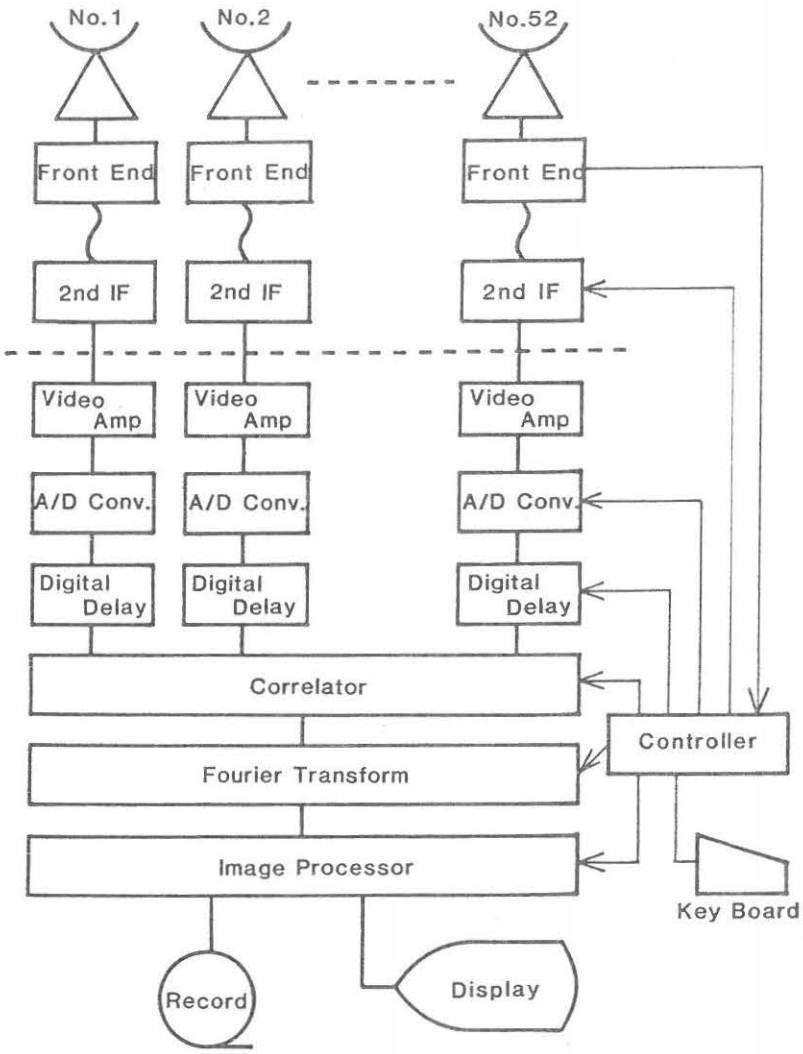

Fig. 1. Block diagram of the proposed system.

one-dimensional or two-dimensional solar brightness distribution. Fourier-transform is performed to obtain the solar brightness distribution from these components. Display and storage of the observed data are performed by a processor named Image Processor. At present, the stages above the dashed line in this figure, i.e. front-end and 2nd IF stage, have been completed in the previous project (Ishiguro et al., 1979). As listed in Table 1, expected bandwidth, time resolution and minimum detectable flux of this new system are 10 MHz, 0.1 sec./image and about 0.5 s.f.u., respectively. In this system, digital correlators and digital delay lines are used because they are superior to analog ones in compactness and case of adjustment.

Operating Frequency (Center Frequency)	3745.8 MHz
Band Width	10 MHz
Hour Angle Coverage	0h ± 2h
Field of View	40' arc× 40' arc
Spatial Resolution (λ/D)	38" arc (E-W One-dimension) 1.25 arc (N-S One-dimension) 2.5 arc×2.5 arc (Two-dimension)
Time Resolution	0.1 sec./image
Minimum Detectable Flux	∿0.5 s.f.u.
Polarization	Right and Left

1 s.f.u.(Solar Flux Unit)= 10^{-22} Watts m^{-2} Hz^{-1}

Table 1. Performance of the new system.

2.1 3rd IF

At 3rd IF stage, the signal transmitted from 2nd IF stage is frequency-converted to videoband signal, and amplified up to a signal level acceptable to A/D converter. There are two types of mixers,-- the single sideband type, and the double sideband type. The former requires composite operations for fringe stopping and delay tracking, but the latter can separate them. The latter needs twice as many correlators as the former to obtain equal sensitivity. To reduce the complexity of operations, the double sideband type is used in the new system.

2.2 A/D Converter and Correlator

As the digital correlator used for radio telescopes, the three-level correlator and the one-bit correlator are relatively familiar. For example, the three-level correlator is used in the Very Large Array (VLA), and one-bit correlator is used in the Westerbork Synthesis Radio Telescope (WSRT) in some cases. Therefore these types of digital correlator are compared in order to decide which type of correlator is appropriate for our system.

Assuming two signals with the same Gaussian amplitude distribution function, cross-correlation between the signals, measured by the theoretically perfect one-bit correlator r_1, the three-level correlator r_2 and the analog correlator r_3, are respectively expressed as

$$r_1 = \frac{2}{\pi}\sin^{-1}\rho \quad , \tag{1}$$

$$r_2 = \pi^{-1}\int_0^{\rho}(1-x^2)^{-1/2}(\exp\{-v_0^2/[\sigma^2(1+x)]\} + \exp\{-v_0^2/[\sigma^2(1-x)]\})dx \quad , \tag{2}$$

and $$r_3 = \sigma^2\rho \quad , \tag{3}$$

where ρ is true correlation between the signals, v_0 is the threshold level of the A/D converter, and σ is rms amplitude of the signals (Hagen and Farley, 1973). The correlation measured by a one-bit correlator does not include the amplitude information of the signals. This means that one-bit correlation is less sensitive to the gain variation of pre-amplifier than the others.

For digital correlators, degradation of signal-to-noise ratio (S/N ratio) occurs because of the loss of amplitude information caused by quantization. It can be expressed by a Degradation Factor (Bowers and Klinglar, 1974). The Degradation Factor is defined as follows,

$$D = \frac{\text{output signal/noise ratio of analog correlator}}{\text{output signal/noise ratio of digital correlator}} . \tag{4}$$

The Degradation Factor of one-bit, three-level and two-bit correlators are 1.571, 1.235 and 1.135, respectively. One-bit correlator has large Degradation Factor. Therefore its sensitivity is less than that of other types. However, comparing the conditions of solar and cosmic radio observations, it is not a severe problem in the former condition because solar radio flux is much stronger than cosmic one. Furthermore, the Degradation Factor is reduced by increasing the sampling rate to receiver bandwidth. If the sampling rate is two times oversampling, that is four times as much as the receiver bandwidth, the Degradation Factor of a one-bit correlator is reduced to 1.35.

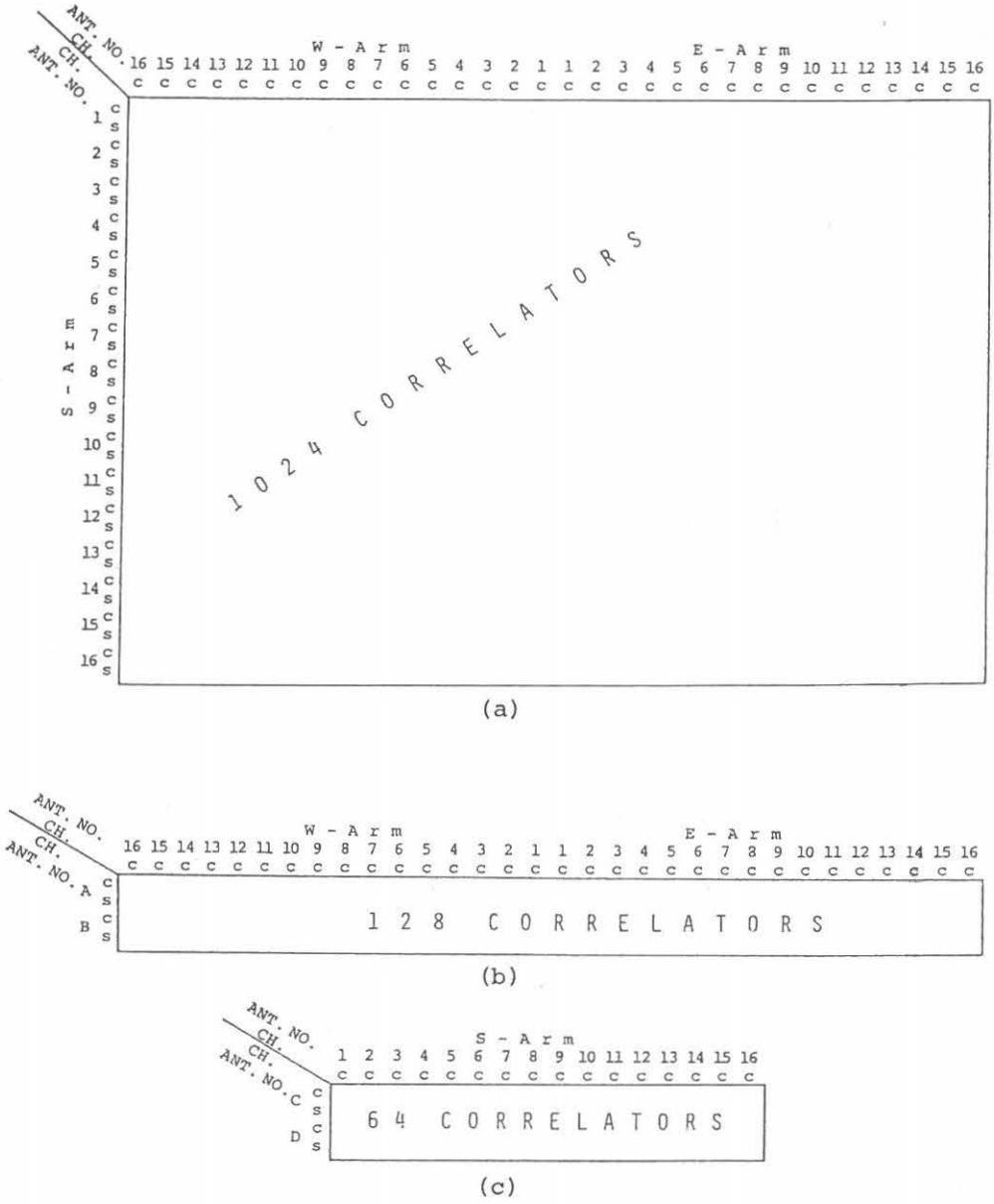

Fig. 2. Correlation diagram of the signals for (a) two-dimensional, (b) E-W one-dimensional and (c) N-S one dimensional observation. If both circular polarizations are measured simultaneously, required correlatiors are twice as many as the numbers shown in this figure.

Considering the above-mentioned merits, a one-bit correlator may be the best of all the types of correlator for the new system.

1024, 128 and 64 correlators are required to form two-dimensional, E-W one-dimensional and N-S one-dimensional images, respectively. Figure 2 indicates antenna combinations required by our system, and also correlations. Another set of correlators is required to measure two circular polarizations simultaneously. In addition, some correlators used for phase correction are required. If the information of the redundancy of fundamental antenna spacing (86.03λ) is used for phase correction, 92 correlators are required.

2.3 Fringe Stopping

Fringe stopping, which compensates a change in the fringe phase caused by the diurnal motion of the sun, is performed by 8-bit digital phase shifters equipped in the 2nd IF stage. Each phase shifter is controlled by the following relations,

$$\phi_{EW} = \frac{2\pi d}{\lambda}\cos\delta\sin H \quad \text{for the E-W baseline,} \tag{5}$$

and

$$\phi_{NS} = -\frac{2\pi d}{\lambda}(\sin\gamma\cos\delta\cos H - \cos\gamma\sin\delta) \quad \text{for the N-S baseline,} \tag{6}$$

where λ is the observation wavelength, d is the distance from the phase center of the T-shaped array, γ is the latitude of the phase center, and δ and H are the declination and the hour angle of the sun. The distance d is defined as positive if it is measured to the east or the south of the phase center and negative if it is measured to the west of the phase center.

2.4 Delay Tracking

The coherency between signals of two antennas is

$$\alpha = \frac{\sin\pi\cdot\Delta t\cdot B}{\pi\cdot\Delta t\cdot B} , \tag{7}$$

where Δt is the relative propagation delay between two signals and B is the bandwidth of receiver. The relative propagation delay is simply

$$\Delta t = \frac{d'\sin\theta}{c} , \tag{8}$$

where d' is the length of the baseline between the two antennas, c is the velocity of propagation, and θ is the angle between the line-of-sight and the plane vartical to the baseline.

Delay lines are used to correct the relative propagation delay and to reduce the loss of coherency. The length of the delay lines must be varied according to the change of the angle θ and therefore the change of the relative propagation delay Δt caused by the diurnal motion of the source.

As the delay line, the cable delay line (analog delay line) and

the digital delay line are available. The former performs the delay tracking by changing the length of signal cable, and the latter by changing the sample timing of A/D converter or the length of shift register. The cable delay line causes gain variation with the delay switching and requires a relatively large space to store the cables. Therefore the digital delay line is used in the new system.

Two kinds of digital delay line are used in the new system. One is a fine delay line, which can switch in step of one fifth of the sampling interval time (50 nano-sec.) and has maximally 5 steps. Another is a coarse delay line, which operates at the sampling frequency. The former can be realized by shifting the relative sample timing of the sampler. The latter can be realized by using a shift register operating at the sampling frequency. Figure 3 indicates the block diagram of the delay line circuit.

If delay correction was performed in the step of $\Delta t'$, equation (7) is modified as follows;

$$\alpha = \frac{\sin\pi(\Delta t - n\Delta t')B}{(\Delta t - n\Delta t')B} \quad , \tag{9}$$

where n=0, ± 1, ± 2, ... Assuming that the bandwidth B is 10 MHz and the step of the delay correction $\Delta t'$ is 10 nano-sec., which are expected in the new system, the loss of coherency may be kept below 2 percents (α=0.983).

Maximum length of the coarse delay line, i.e. the length of shift register L, is defined as follows;

$$L = [\Delta t_{max} \cdot f_s] + 1 = [\frac{d' \sin\theta_{max}}{c} \cdot f_s] + 1 \quad , \tag{10}$$

where f_s is sampling frequency, θ_{max} is the maximum value of the angle , and [ ] is the Gauss' notation. If fs= 20 MHz and θ_{max}= 30 deg., the length for the longest E-W baseline of the array (d'= 436.88 m) is 15.

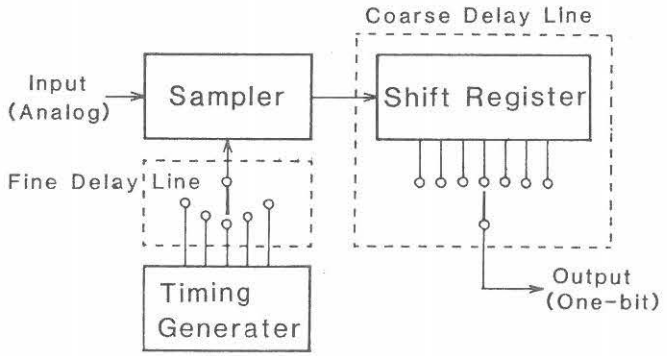

Fig. 3. Schematic block diagram of delay line circuit. Fine delay is performed by shifting the timing of the sample clock. Coarse delay is performed by changing the length of the shift register.

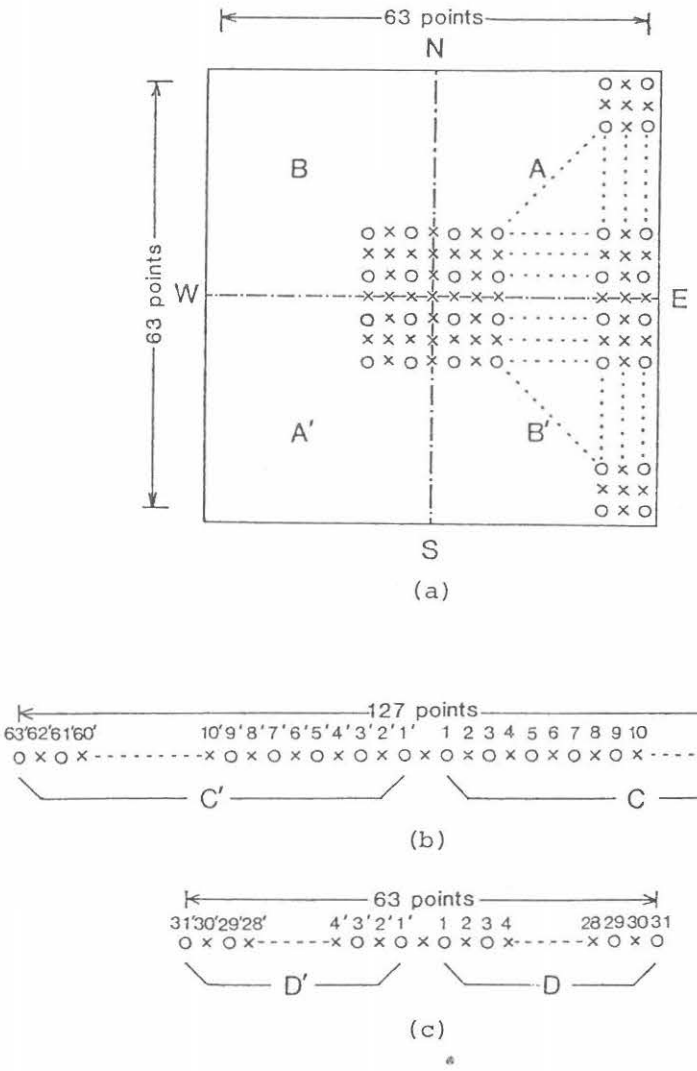

Fig. 4. Distribution of the spatial frequency component obtained by the proposed system. (a) Two dimension. (b) E-W one dimension. (c) N-S one dimension.

(1) A, A', B, and B' are two-dimensional complex matrices with 31×31 elements.

(2) C and C' are one-dimensional complex matrices with 63 elements.

(3) D and D' are one-dimensional complex matrices with 31 elements.

(4) A', B', C' and D' are respectively complex conjugates to A, B, C and D.

2.5 Fourier Transform and Image Processor

The correlations which can be obtained by the array configuration of the λ 8-cm radioheliograph are odd components on the spatial frequency domain (u-v plane) as shown in Figure 4. 128-point, 64-point and 64×64-point discrete Fourier transforms are needed to produce E-W one-dimensional, N-S one-dimensional and two-dimensional solar images, respectively. If we expect to see the solar image with 0.1 second time-resolution in real time, these Fourier transforms are processed within 0.1 second.

If the new system is operated for four hour a day, the amount of the data produced by the new system is about 380 Mega-data a day, and it is four orders greater than that of the present system (about 25 kilo-data). The image processor is used to compress and store this large amount of data efficiently, and to reduce the work of the operator. At present, the most appropriate medium may be videotapes or videodisks to store such a large amount of data

3. Expriments of One-bit Correlator

In the new system, a large number of correlators are used. Therefore we construct a test circuit of one-bit correlator and investigate the characteristics of one-bit correlator. Block diagram of the test circuit is illustrated in Figure 5. This test circuit has a function to obtain a cross-correlation of a pair of input analog signals, which are taken out from the monitor terminals equipped at the 2nd IF stage. The input signals are amplified and frequency-converted to videoband signals. At the sampling stage, the

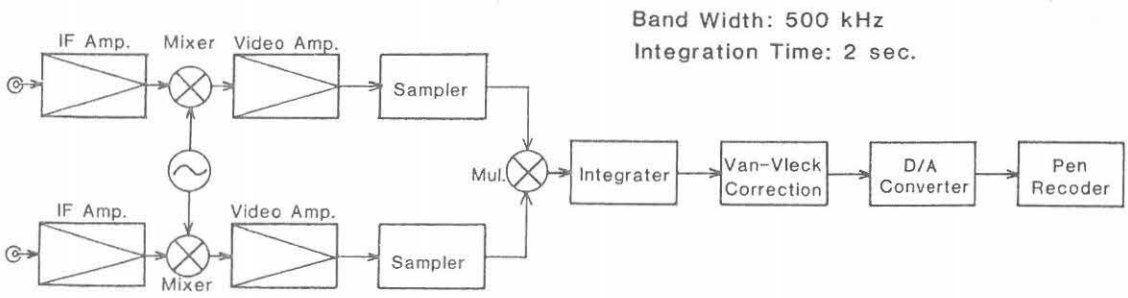

Fig. 5. Block diagram of test circuit.

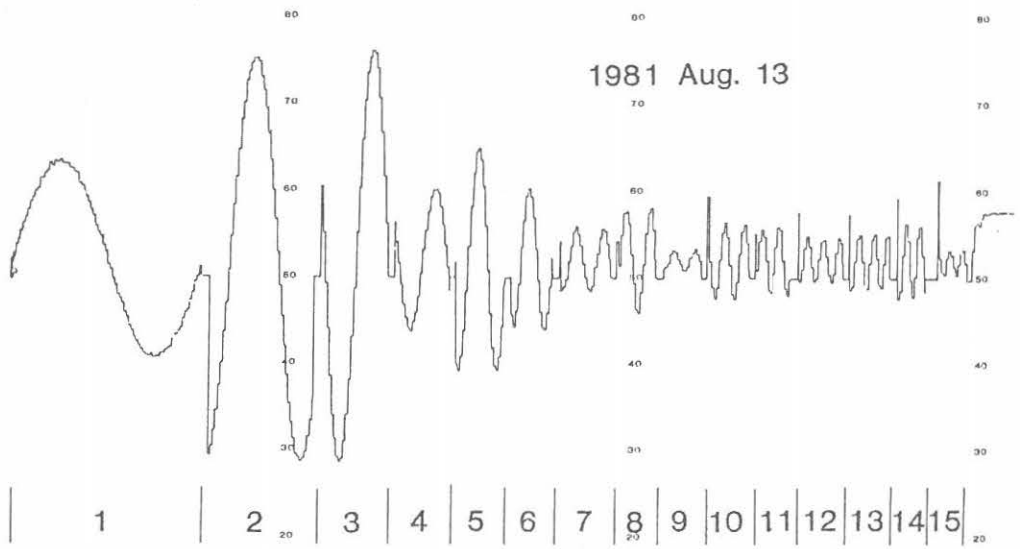

Fig. 6. Fringe pattern for various baseline lengths measured by the test circuit. The numbers below the patterns represent multiples to the unit antenna spacing. West arm of the T-shaped array is used in this measurement.

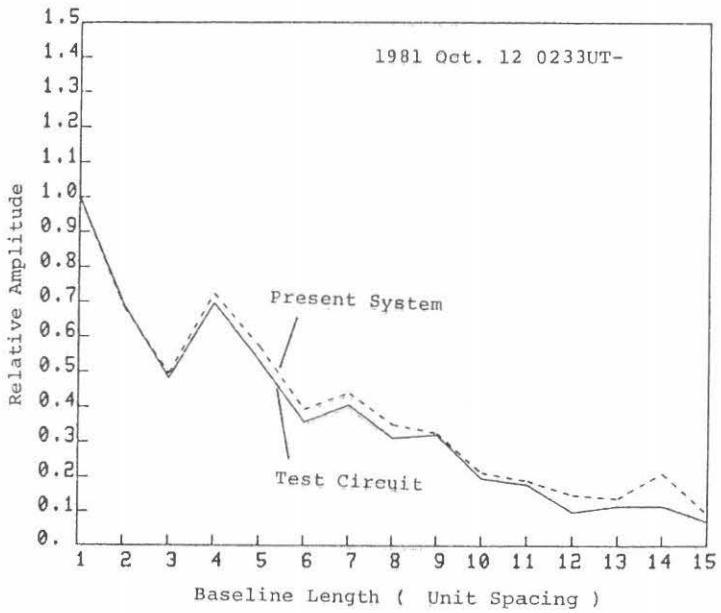

Fig. 7. Visibility plots to baseline length. Full line and broken line represent the results obtained by the test circuit and the present λ 8-cm radioheliograph system, respectively. Visibility amplitude is normalized by the value for unit antenna spscing.

signals are converted to one-bit digital signals which retaine only polarity information. The one-bit correlator is composed of an exclusive-OR circuit and a synchronous counter. The former performs one-bit multiplication of its input signals. The latter integrates the resultant signal over an arbitrary period. As one-bit correlation and true correlation have a relationship expressed in equation (1), transform from the former to the latter is performed by the Van Vleck correction circuit, which is constructed by the read only memory (ROM). Finally, the corrected data is recorded on a chart-recorder through digital-to-analog converter.

The test circuit has relatively narrow bandwidth (500 kHz), slow sample rate (1.2 MHz), and long integration time (about 2 sec.). This circuit does not have enough performance to use in the new system, but we could draw out some interesting information to design the proposed system.

A set of the fringe pattern for W-arm of the T-shaped array measured by the test circuit is given in Figure 6. Baseline lengths for the fringes are from 1 to 15 times the unit antenna spacing. These fringes correspond to spatial frequency components from fundamental to the 15th harmonic of one-dimensional solar map observed at the same time.

Visibility amplitude obtained by the test circuit is compared with that obtained by the present λ 8-cm radioheliograph system. An example of the visibility plots as a function of the baseline length is shown in Figure 7. It is to be noted that both plots in this figure show similar profile. From this experiment, it becomes clear that true visibility for the solar brightness distribution can be obtained by the one-bit correlator.

An example of the fringe pattern for bursts measured by the test circuit is shown in Figure 8. The antenna spacing used is nine times the unit antenna spacing. In this figure, two bursts of short duration can be seen. The first one represents the increase of the visibility amplitude, but the second one represents the decrease. It means that the solar brightness distribution was rapidly changing during the bursts. Time profiles of these bursts are observed by the 3.75 GHz fully-automatic radiopolarimeter at Toyokawa (Figure 8(b)).

The data obtained by these experiments are not treated quantitatively, but it become clear that a one-bit correlator can be used in the new system. At present, we are constructing a proto-type circuit of the correlator to be used in the new system, which has the bandwidth of 10 MHz, the sampling rate of 20 MHz and the integration

time of 0.1 sec. The circuit configuration is as same as that of the test circuit mentioned above. Using this circuit, we will quantitatively investigate the characteristics of the proto-type circuit, such as dynamic range or stability.

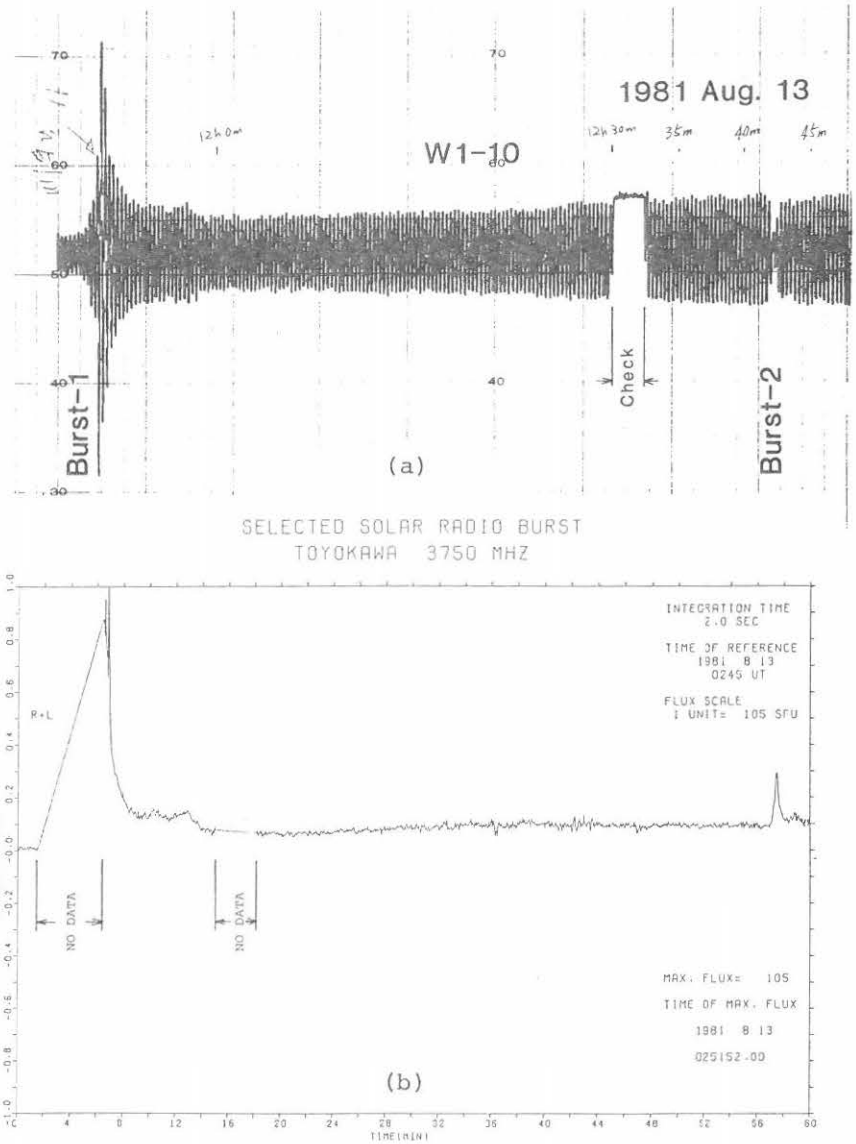

Fig. 8. (a) Fringe pattern for the bursts measured by the test circuit. Two remarkable bursts with fast time variation are seen in this figure. Gradual variation of the visibility amplitude is caused by the change of baseline projection to the sun and a GRF burst. (b) Time profile of the same bursts measured by the 3.75 GHz fully-automatic radiopolarimeter.

References

Bowers, F.K., and Klingler, R.J.: Quantization Noise of Correlation Spectrometers, Astron. Astrophys. Suppl., 15, 373 (1974).

Hagen, J.B., and Farley, D.T.: Digital-correlation Techniques in Radio Science, Radio Science, 8, 775 (1973).

Ishiguro, M., Tanaka, H., Enome, S., Torii, C., Tsukiji, T., Kobayashi, S., and Yoshimi, N.: 8-CM Radioheliograph, Proc. Res. Inst. Atmospherics, Nagoya Univ., 22, 1 (1975).

Ishiguro, M., Torii, C., Shibasaki, K., Enome, S., and Tanaka, H.: A Project to Improve the Sensitivity and the Phase Stability of the λ 8-CM Radioheliograph at Toyokawa, Proc. Res. Inst. Atmospherics, Nagoya Univ., 26, 145 (1979).

Ishiguro, M., Enome, S., Shibasaki, K., and Tanaka, H.: Observation of the Quiet Sun during the Solar Minimum (Cycle 20-21) with the Toyokawa λ 8-cm Radioheliograph, Publ. Astro. Soc. Japan, 32, 533 (1980).

Itoh, Y., and Torii, C.: Phase Adjustment of the Improved λ 8-cm Radioheliograph, Proc. Res. Inst. Atmosphericcs, Nagoya Univ., 28, 49 (1981).

Naito, Y.: Phase Stability of the New Local Oscillator System for the λ 8-CM Radioheliograph at Toyokawa, Proc. Res. Inst. Atmospherics, Nagoya Univ., 26, 67 (1979).

Shibasaki, K., Ishiguro, M., Enome, S., Tanaka, H., Torii, C., Tsukiji, Y., Kobayashi, S., and Yoshimi, N.: λ 8-cm Radioheliograms, Proc. Res. Inst. Atmospherics, Nagoya Univ., 23, 21 (1976).

Shibasaki, K., Ishiguro, M., Enome, S., and Tanaka, H.: A Colonal Hole Observed with a λ 8-cm Radioheliograph, Publ. Astro. Soc. Japan, 30, 589 (1978).

Tanaka, H., Enome, S., Torii,C., Tsukiji, Y., Kobayashi, S., Ishiguro, M., and Arisawa, M.,: 3-cm Radioheliograph, Proc. Res. Inst. Atmospherics, Nagoya Univ., 17, 57 (1970).

Torii, C., Tsukiji, Y., Kobayashi, S., Yoshimi, N., Tanaka, H., and Emone, S.: Full-Automatic Radiopolarimeters for Solar Patrol at Microwave Frequency, Proc. Res. Inst. Atmospherics, Nagoya Univ., 26, 129 (1979).